

## Aspect Ratio Dependence in Reactor Design is not Monotonic Thus Leading to an Optimization Problem

There are many perceived benefits of going to low aspect ratio for tokamak reactor concepts, such as increased stability limits (beta, elongation) and potentially larger bootstrap fraction, all in a device at smaller major radius (i.e. more compact).

However, these potential benefits must be balanced by the reduction in achievable on-axis magnetic field, the need for inner wall shielding and central solenoid, and the potentially larger mechanical stresses in a tighter configuration.

In this work, we aim to clarify how the role of aspect ratio enters OD design studies using various assumptions on:

- The target mission (high power net-electric DEMO, low power net electric Pilot Plant, high neutron fluence FNSF)
- Stability and confinement physics  $\Rightarrow \beta_N, \kappa, H$
- Magnet technology (HTS, LTS, copper)  $\Rightarrow B_{max}, J_{WP}, \sigma_{max}$
- Heating & current drive technology (RF, NBI)

## The Overarching Structure of our Implemented Problem Solving Method

A code was developed for this design study that is capable of solving assuming either fixed  $P_f$  or fixed  $P_{ext}$ .

The cases presented then assume:

- 100% non-inductive operations
- Confinement is performing at:
  - The  $\beta_N$  limit scaled as  $\beta_N = 3.12 + \epsilon^{1.7}$  [6]
  - 5% below the elongation limit scaled as  $\kappa = 1.9 + 1.9\epsilon^{1.4}$  [6]

As such, the two above cases can be formulated into nonlinear system of equations derivable in the form of:

- $f_{bs} + f_{CD} = 1$ , from 100% non-inductive assumption
- $n_{He} = 0.0106 \frac{\beta_N B T_0 I_p}{a \left(1 + \frac{5}{Q_p} f_{rad}\right) \tau_E}$ , from combining simple, steady-state helium and energy transport equations [11]

## Resultant System of Equations

<p>Fixed <math>P_f</math> case --</p> $F(N, I_p) = \frac{1}{2}[n_e(I_p) - N] - \frac{0.0106 \beta_N B T_0 \tau_a}{a \tau_E I_p} \left[ 1 + \frac{5}{Q_p(N, I_p)} - f_{rad}(N, I_p) \right] = 0 \quad (1)$	<p>Fixed <math>P_{ext}</math> case --</p> $F(N, I_p) = \frac{1}{2}[n_e(I_p) - N] - \frac{0.0106 \beta_N B T_0 \tau_a}{a \tau_E I_p} \left[ 1 + \frac{5}{Q_p(N, I_p)} - f_{rad}(N, I_p) \right] = 0 \quad (5)$
---	---

<p><math>G(N, I_p) = P_f - \frac{1}{4} N^2 \langle \sigma v \rangle E_f V = 0 \quad (2)</math></p>	<p><math>G(N, I_p) = I_p - \frac{1}{2} \left[ c_{bs}(I_p) 0.25 \beta_N \sqrt{\epsilon a B T_0 S} + \left( c_{bs}(I_p) 0.25 \beta_N \sqrt{\epsilon a B T_0 S} \right)^2 + 4 \eta_{CD}(N, I_p) \frac{P_{ext} \pi a^2}{f_{GW} R_0} \right]^{1/2} = 0 \quad (6)</math></p>
--	--

<p><math>\frac{1}{Q_p(N, I_p)} = \frac{1}{P_f} \left[ I_p - c_{bs}(I_p) 0.25 \beta_N \sqrt{\epsilon a B T_0 S} \right] n_e(I_p) \frac{R_0}{\eta_{CD}(N, I_p)} \quad (3)</math></p>	<p><math>Q_p(N, I_p) = \frac{1}{P_{ext}} \frac{1}{4} N^2 \langle \sigma v \rangle E_f V \quad (7)</math></p>
<p><math>f_{rad}(N, I_p) = \frac{P_{br}(N, I_p) + P_{syn}(N, I_p)}{P_\alpha} + f_{rad, imp} \quad (4)</math></p>	<p><math>f_{rad}(N, I_p) = \frac{P_{br}(N, I_p) + P_{syn}(N, I_p)}{P_\alpha} + f_{rad, imp} \quad (8)</math></p>

## Outline of Simple TF Coil Model We Used

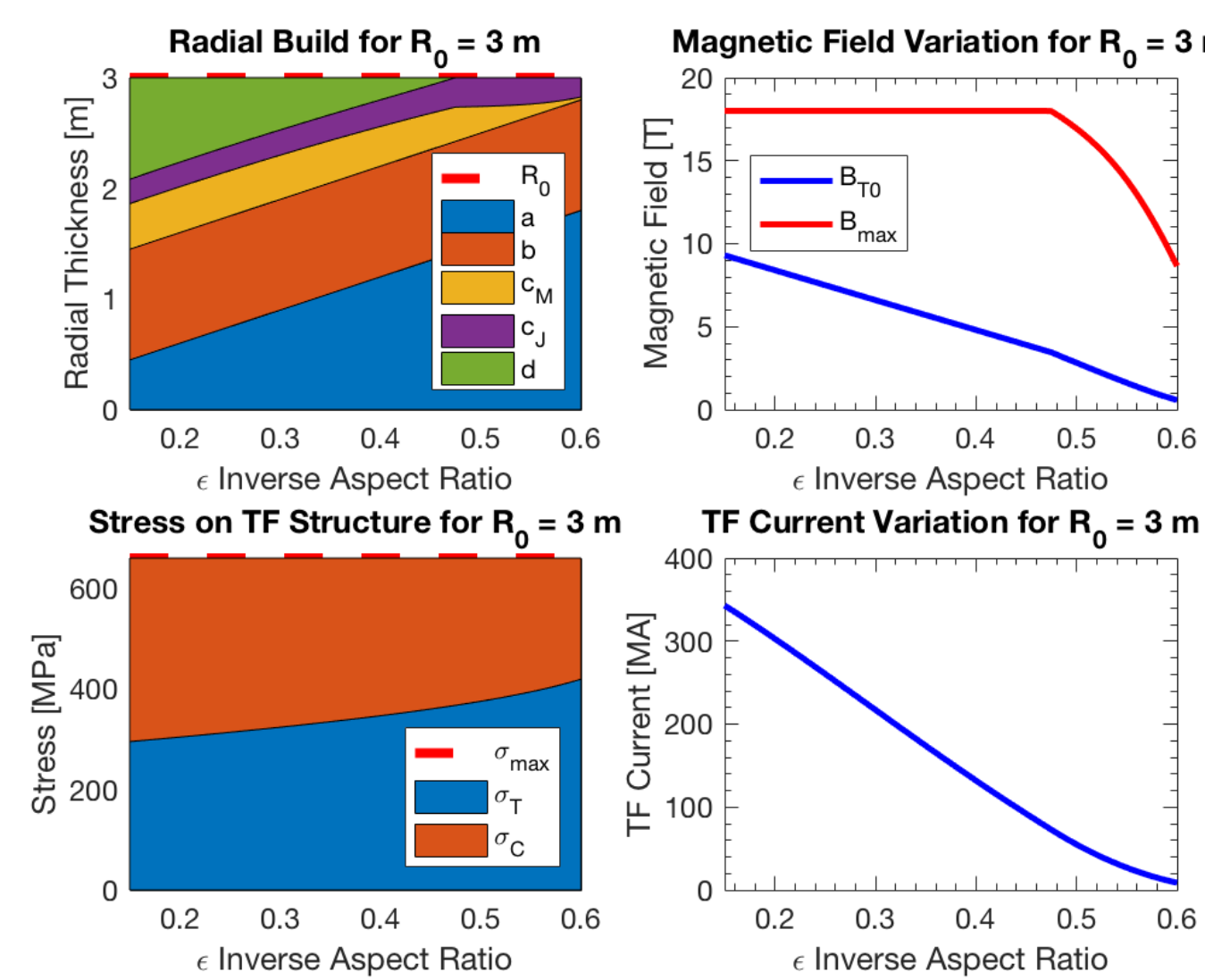
The design of the toroidal field (TF) coils are a principle design component of a tokamak reactor that drive plasma performance.

As such, we apply a simple coil model as described in Freidberg 2015 [7].

- Assume rectangular cross-sections in wedging contact on the inboard side.
- The thickness of the structural material,  $c_M$ , can be obtained by balancing magnetic forces to the maximum allowable stress of the material.
  - Tensile (z-direction)
  - Compressive (r-direction)
- The thickness of the winding pack,  $c_J$ , can be obtained by applying Ampère's Law on the inboard leg.

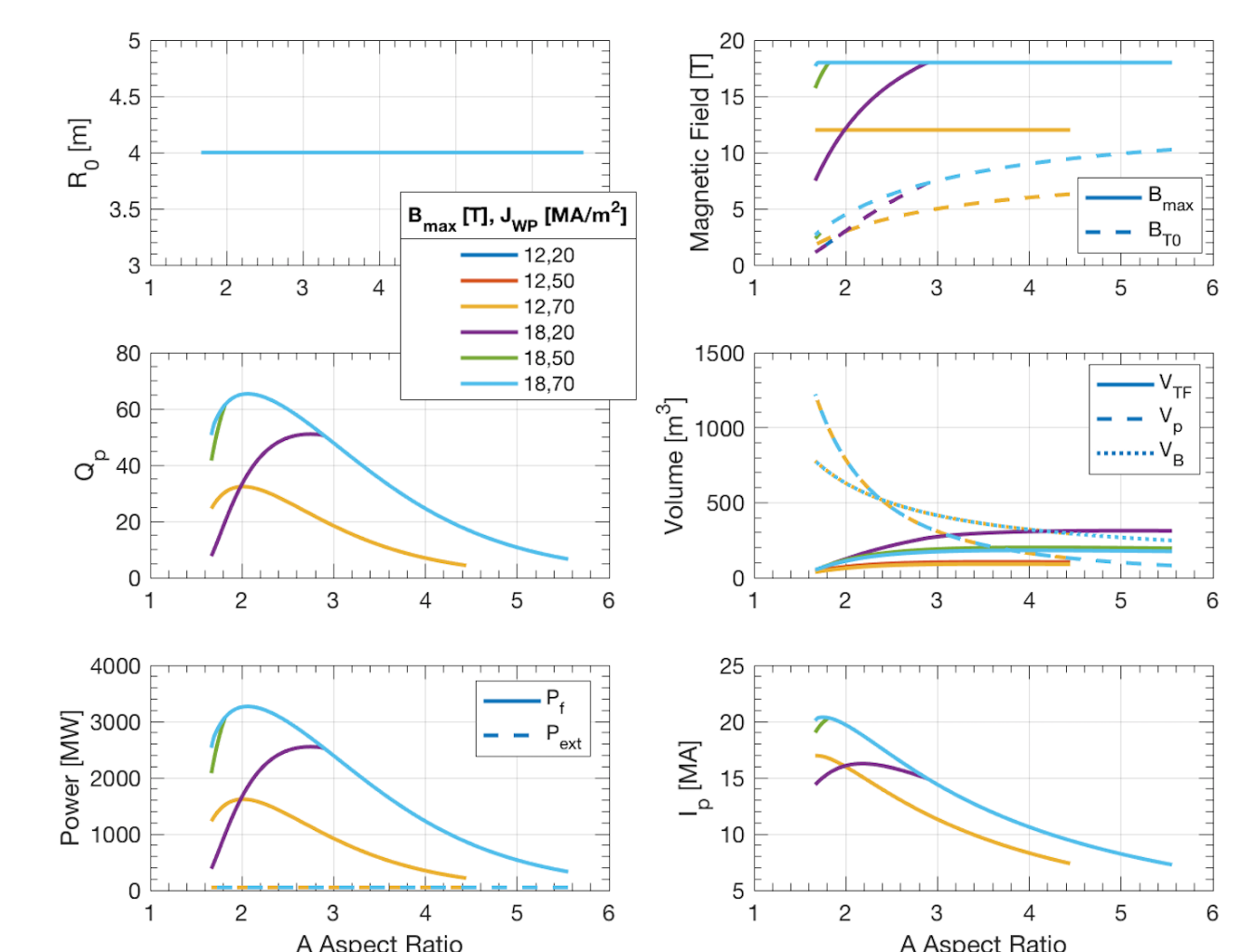
The performance of the magnets can therefore be calculated by prescribing  $B_{max}, J_{WP}, \sigma_{max}$  to values characteristic to HTS, LTS, or Cu coils.

## Example of Magnet Performance over Aspect Ratio



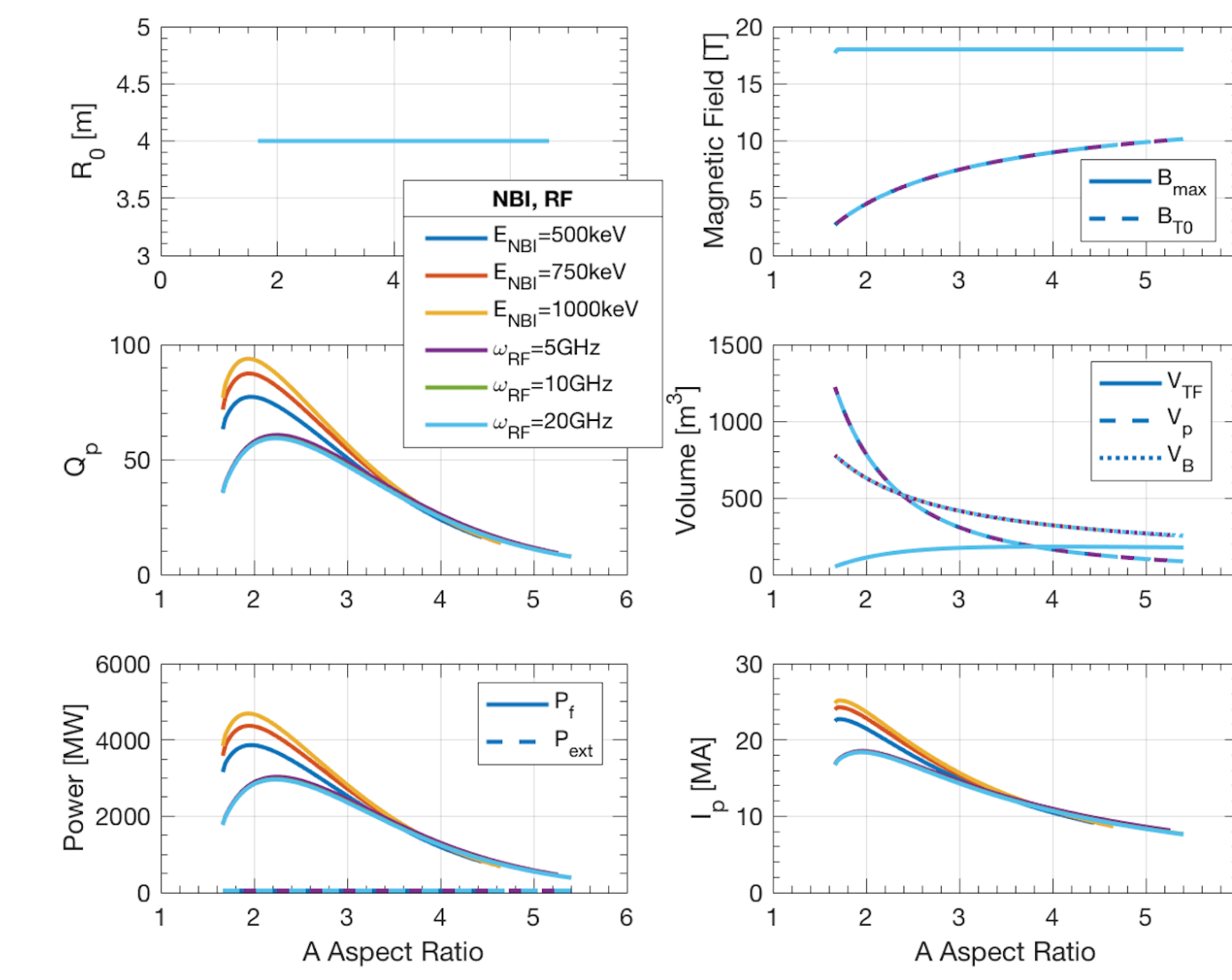
- Presented is characteristic of REBCO magnets with  $\sigma_{max} = 660 MPa$  and  $b = 1.0m$ 
  - $B_{max} = 18T$
  - $J_{WP} = 70 \frac{MA}{m^2}$
- Note that  $B_{max}$  was needed to be derated to maintain  $R_0 - a - b - c_J - c_M \geq 0$ , where  $b$  is the blanket thickness (Breeder+Shield).
- $d$  is the remaining space for an ohmic heating (OH) coil.
- It can be seen that as  $A \rightarrow 1$ , the need for 100% non-inductive start-up and ramp-up increases.

## Optimizing Magnet Technology by Varying $B_{max}, J_{WP}$



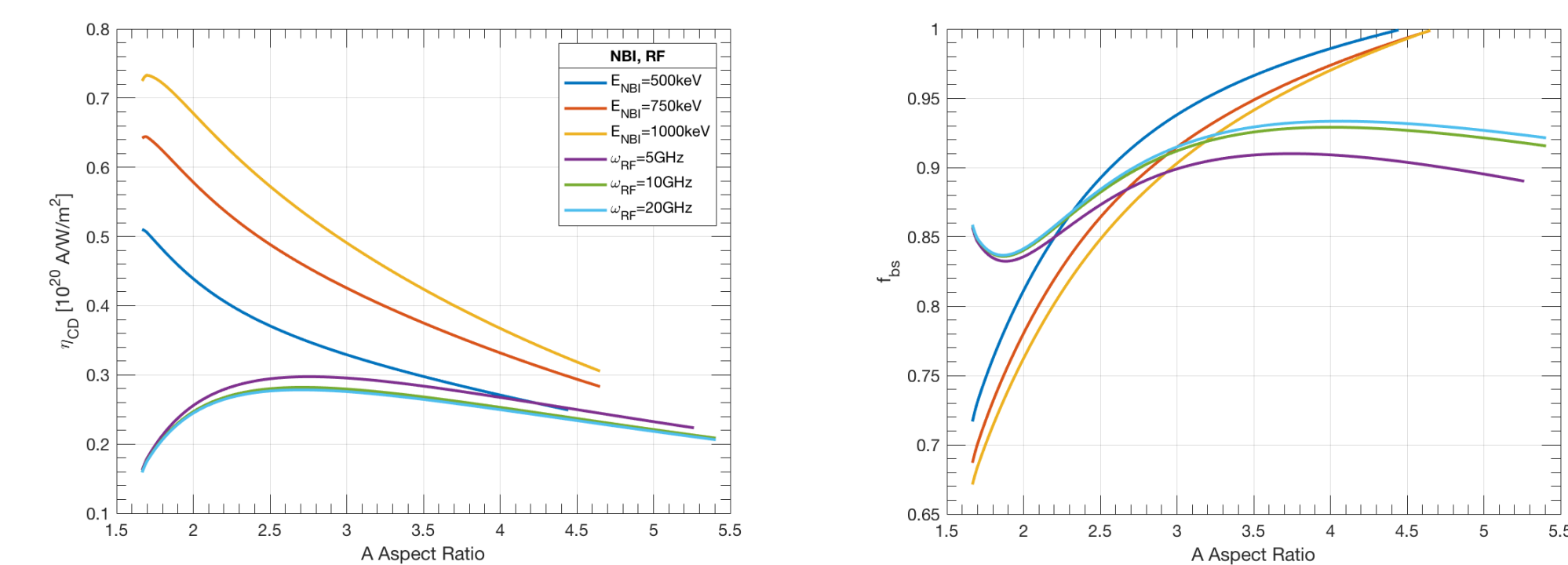
- Presented is the case of fixed  $P_{ext} = 50MW$  at  $R_0 = 4m$ .
- Increasing  $B_{max}$  significantly increased performance for every reactor size.
- Though doing this causes greater magnetic forces and thus a need for  $c_M \uparrow$ .
- This is mitigated by increasing  $J_{WP}$  ( $c_J \downarrow$ ) thus relaxing inboard constraints.
- This allowed for increased performance at lower aspect ratio.

## Perferable Aspect Ratio for RF and NBI Current Drive Technology with Varying $\omega_{RF}$ and $E_{NBI}$



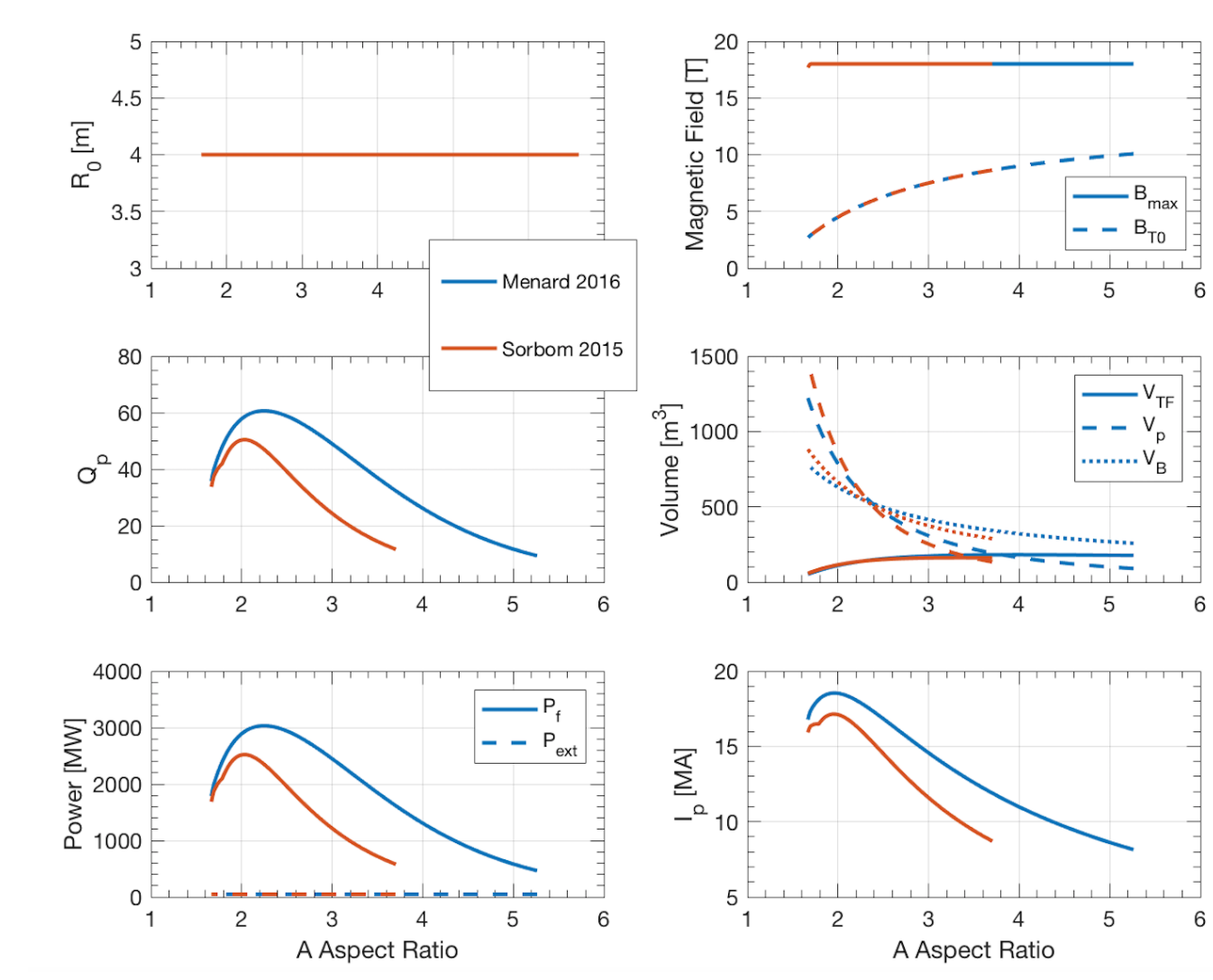
- Presented is the case of fixed  $P_{ext} = 50MW$  at  $R_0 = 4m$ .
- With an RF current drive scheme, the plasma approaches the over-dense ( $f_{ce} > 1$ ) limit as  $A \rightarrow 1$  causing  $\eta_{CD} \downarrow$ .
- With a NBI current drive scheme,  $\eta_{CD}$  contrarily decreases with  $A \uparrow$  as  $T_e \downarrow$  and  $n_e \uparrow$ .
- This interplay causes NBI to be optimized at low aspect ratio and vice versa for RF.

## Investigating How these two Current Drive Schemes Differed, Particularly at Low Aspect Ratio



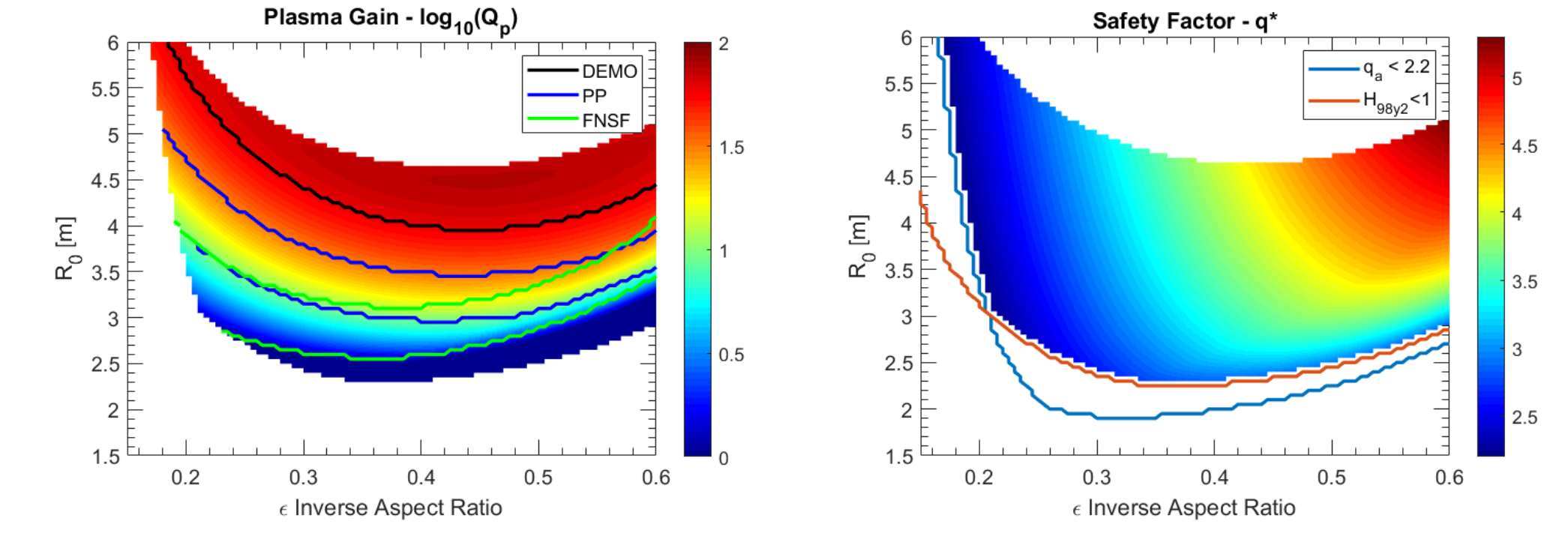
- Considering the presented  $I_p$  and  $f_{bs}$  graphs, the total bootstrap current of the cases hardly changed at low aspect ratio.
- As such, the higher performance of the NBI cases is merely due to the increased efficiency in converting 50MW into plasma current.

## Improvement in Performance from Less Conservative Assumptions on Stability Physics



- Presented is the case of fixed  $P_{ext} = 50MW$  at  $R_0 = 4m$ .
- The  $\beta_N(A)$  and  $\kappa(A)$  scalings presented in Sorbom 2015 are more conservative than those applied thus far [1].
  - $\beta_N = 3$
  - $\kappa = 5.4\epsilon$
- This decrease in stability physics caused a notable decrease in performance for every reactor size.

## General Optimization of Machine with $P_{ext} = 50MW$



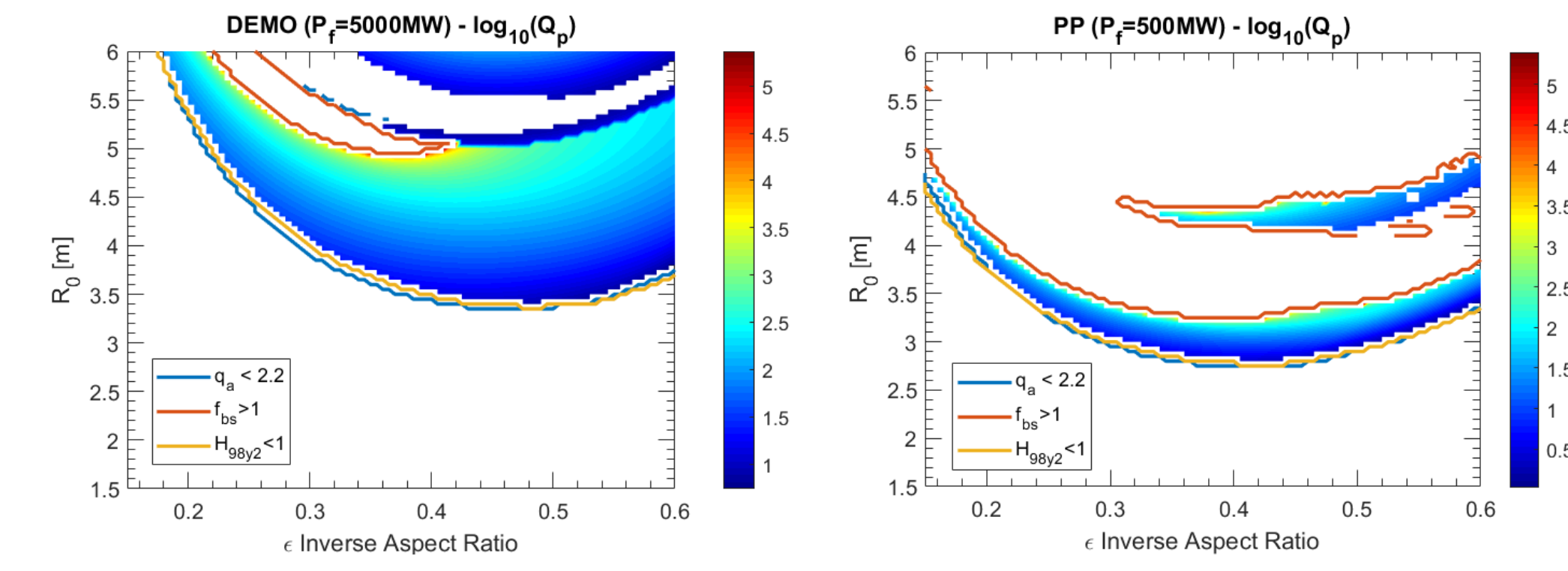
There exists different classes of machines whose target properties affect optimization with reactor space. These classes have been defined as follows:

- DEMO --  $3000 \leq P_f \leq 6000 MW, Q_p \geq 10$
- PP --  $300 \leq P_f \leq 1500 MW, Q_p \geq 10$
- FNSF --  $0.5 \leq W_n \leq 2.5 \frac{MJ}{m^2}$

Presented is a general representation of where those machines would sit in reactor space given fixed  $P_{ext} = 50MW$ .

Simple constraints on reasonably achievable stability, confinement, and current properties were applied.

## General Optimization of Machine with Fixed $P_f$



- Again, simple constraints on stability, confinement, and current properties were applied.
- It can be seen that targeting a DEMO would favor machines with larger aspect ratio.
- Targeting a PP would more so favor a mid-range aspect ratio of  $A \approx 2$ .

## Conclusions

- The general results of our optimization showed there is much to gain at lower aspect ratio.
  - $A \approx 2$ , much lower than most current large tokamak experiments.
- Magnet technology increased reactor performance at lower aspect ratio, higher  $B_{max}$ , and higher  $J_{WP}$ .
  - Though this increases constraints on the inboard radial build.
  - Therefore, greater need for non-inductive start-up and ramp-up.
- There is a notable distinction in aspect ratio where one would prefer RF or NBI current drive schemes.

## References

- [1] B. N. Sorbom, J. Ball, T. R. Palmer, et al., "ARC: A Compact, High-Field, Fusion Nuclear Science Facility and Demonstration Power Plant with Demountable Magnetics", *Fusion Engineering and Design*, Volume 10, 2015, pp. 378-405.
- [2] D. H. Start, J. G. Cordey, and E. M. Jones, "The Effect of Trapped Electrons on Beam Driven Currents in Toroidal Plasmas", *Plasma Physics*, Volume 22, Number 4, 1980, pp. 303-316.
- [3] D. Whyte, "The Science Case for High Field Fusion", *59th Annual Meeting of the APS Division of Plasma Physics*, American Physical Society Division of Plasma Physics, 27 October 2017, Milwaukee, WI. Conference Presentation.
- [4] H. S. Bosch, and G. M. Hale, "Improved Formulas for Fusion Cross-Sections and Thermal Reactivities", *Nuclear Fusion*, Volume 32, Number 4, 1992, pp. 611-631.
- [5] J. E. Menard, "Compact Steady-State Tokamak Performance Dependence on Magnet and Core Physics Limits", *Nuclear Fusion*, Submitted 2018.
- [6] J. E. Menard, T. Brown, L. El-Guebaly, et al., "Fusion Nuclear Science Facilities and Pilot Plants Based on the Spherical Tokamak", *Nuclear Fusion*, Volume 56, Number 10, 2016.
- [7] J. P. Freidberg, F. J. Mangiarotti, and J. Minervini, "Designing a Tokamak Fusion Reactor—How Does Plasma Physics Fit In?", *Physics of Plasmas*, Volume 22, 2015.
- [8] J. Wesson, *Tokamaks*, 3rd ed., Oxford University Press, 2004.
- [9] M. N. Rosenbluth, "Synchrotron Radiation in Tokamaks", *Nuclear Fusion*, Volume 10, Number 3, 1970, pp. 340-344.
- [10] R. J. Thome, and J. M. Tarrh, *MHD and Fusion Magnets: Field and Force Design Concepts*, John Wiley & Sons, 1982.
- [11] S. C. Jardin, C. E. Kessel, D. Meade, and C. L. Neumeyer, "System Analysis of a Compact Next Step Burning Plasma Experiment", *Fusion Science and Technology*, Volume 43, Number 2, 2002, pp. 161-175.